

Baryon masses in the three-state Potts field theory in a weak magnetic field

S. B. Rutkevich

Fakultät für Physik, Universität Duisburg-Essen, D-47058 Duisburg, Germany

E-mail: sergei.rutkevich@uni-due.de

Abstract. The 3-state Potts field theory describes the scaling limit of the 3-state Potts model on the two-dimensional lattice near its continuous phase transition point. In the presence of thermal and magnetic field perturbations, the 3-state Potts field theory in the ordered phase exhibits confinement of kinks, which allows both mesons and baryons. We calculate the masses of light baryons in this model in the weak confinement regime in leading order of the small magnetic field. In leading order of perturbation theory, the light baryons can be viewed as bound states of three quantum particles - the kinks, which move on a line and interact via a linear potential. We determine the masses of the lightest baryons by numerical solution of the associated non-relativistic one-dimensional quantum three-body problem.

1. Introduction

Confinement of kink topological excitation is a quite common phenomenon in $2d$ -Euclidean Quantum Field Theories (QFT), which are invariant under some discrete symmetry group, and display a continuous order-disorder phase transition. After the Wick rotation, such models can be also viewed as relativistic QFT with one space and one time dimension. If the system has q degenerate vacua $|0_\alpha\rangle$, $\alpha = 1, \dots, q$, in the ordered phase due to the spontaneous breaking of the discrete symmetry, the particle sector of the theory should contain kinks $K_{\alpha\beta}$, $\alpha, \beta = 1, \dots, q$ that interpolate between any two different vacua. The application of a uniform external field that shifts to a lower value the energy of the vacuum $|0_q\rangle$, lifts the degeneracy between the vacua. As a result, the vacuum $|0_q\rangle$ transforms into the true ground state, whereas the states $|0_\alpha\rangle$ with $\alpha = 1, \dots, q-1$ become the non-stable false vacua. This induces a long-range attractive interaction between kinks, which, in turn, leads to their confinement: isolated kinks do not exist in the system any more and become bound into compound particles. Particular realizations of this scenario in different two-dimensional field-theoretical models have been attracted much attention in the recent years [1, 2, 3, 4, 5, 6, 7].

The interest on the problem of kink confinement stems from several origins. First, together with particle decay, inelastic scattering and resonances [8, 9], nucleation in the false vacua etc. [2, 10, 11, 12], this phenomenon falls into the realm of non-integrable aspects of the quantum field theory and statistical mechanics, which cannot be described

within the framework of exactly solvable models. If one views quantum field theories as points in the "space of local interactions" [13, 14] that flow under the action of the renormalisation group, a generic point in this space would correspond to some non-integrable model. The famous example is the near-critical two-dimensional Ising model with non-zero magnetic field [2, 11]. Of course, any progress in understanding universal properties of such non-integrable models is highly desirable.

The second motivation comes from particle physics due to certain common features between confinement of kinks and confinement of quarks in QCD. One example is provided by the Bethe-Salpeter equation introduced in the Ising field theory by Fonseca and Zamolodchikov [2], which turns out to be very similar to the Bethe-Salpeter equation in 't Hooft's multicolor two-dimensional QCD [15], see [3, 16]. Note, that the kinks and their bound states in the confinement regime are often referred to as quarks, mesons (two-kink bound states) and baryons (three-kink bound states), respectively.

Finally, the kink confinement can be realized in one-dimensional condensed-matter systems. It has recently been experimentally observed [17, 18] in the one-dimensional Ising spin-chain ferromagnet cobalt niobate (CoNb_2O_6). The magnetic structure of this compound can be described by the one-dimensional quantum Ising spin-chain model, which is the paradigmatic model for the theory of quantum phase transitions [19].

The simplest and most studied example of kink confinement is provided by the Ising Field Theory (IFT), i.e. the Euclidean QFT, which describes the scaling limit of the two-dimensional lattice Ising model. At zero magnetic field $h = 0$ in the ferromagnetic phase $T < T_c$, this model is characterized by a spontaneously broken \mathbf{Z}_2 symmetry, has $q = 2$ degenerate vacua, and two types of kinks $K_{1,2}$ and $K_{2,1}$, which can be viewed as non-interacting fermions of mass $m \sim (T_c - T)$. Only mesonic bound states are present in this model in the confinement regime, when a magnetic field h that explicitly breaks the \mathbf{Z}_2 symmetry is applied. As $h \rightarrow 0$, the masses $\mu_n(h)$, $n = 1, 2, \dots$, of the mesons densely fill the interval $[2m, \infty)$. The evolution of the IFT meson masses $\mu_n(h)$ with increasing h has been studied in great details both numerically and analytically [20, 2, 3, 4, 21]. Two asymptotic expansions have been obtained for the IFT meson masses in the weak confinement regime $h \rightarrow 0$. The *semiclassical expansion* [3, 4] in integer powers of h holds for the masses $\mu_n(h)$ of highly excited mesons, with $n \gg 1$. The *low energy expansion* [20, 2, 3] in fractional powers of h describes the masses of mesons with not very large values of n , such that $\mu_n(h) - 2m \ll m$. Note, that the leading term of the low energy expansion can be obtained in a very simple manner from the McCoy-Wu scenario, in which the meson is interpreted as a bound state of two non-relativistic quantum particles moving on a line and attracting one another with a linear potential.

The next, richer and more complicated example of the model exhibiting kink confinement is given by the q -state Potts field theory. Being defined in two space-time dimensions only for $q \leq 4$, it represents the scaling limit of the two-dimensional q -state lattice Potts model [22] near its continuous phase transition point. At zero magnetic field $h = 0$, the model is invariant under the group S_q describing permutations of q

colors and has q degenerate vacua in the ordered phase. The PFT reduces to the IFT at $q = 2$. The kinks $K_{\alpha\beta}$, $\alpha, \beta = 1, \dots, q$, are massive particles that interact with each other at short distances already when $h = 0$, if $q > 2$. Interaction of kinks in the $h = 0$ PFT is described by a factorizable scattering matrix, as found by Chim and Zamolodchikov [23]. Application of the magnetic field in the ordered phase leads to kink confinement in the PFT, which has been studied in several papers [5, 24, 25]. The symmetry analysis of the kink bound states, and the qualitative analysis of the evolution of their mass spectrum were performed by Delfino and Grinza [5]. These authors have shown, that besides the mesons, also the baryonic (three-kink) bound states are present at $q = 3, 4$, and the 'tetra-quark' (four-kink) bound states appear at $q = 4$ in the q -state PFT in the confinement regime. Lepori, Tóth, and Delfino [24] have numerically studied the evolution of the particle mass spectrum in the 3-state PFT under variation of the temperature and magnetic field by means of the Truncated Conformal Space Approach (TCSA) [26, 27]. Analytic perturbative analysis of the meson mass spectrum in the q -state PFT has been done in paper [25], in which the leading terms of the both low-energy and semiclassical asymptotical small- h expansions for the meson masses were obtained.

The purpose of the present paper is to calculate the masses of several lightest baryons in the 3-state PFT in the weak confinement regime at $h \rightarrow +0$. Following the McCoy-Wu scenario, we treat the light baryons at $h \rightarrow +0$ as bound states of three non-relativistic quantum particles (the kinks), which move on a line and interact with each other with the linear attractive potential. This allows us to relate the masses of light baryons with discrete energy levels of a certain one-dimensional quantum three-body problem, which we approximately solve by numerical means.

The paper is organized as follows. Section 2 contains a brief introduction into the Potts field theory and some of its well-known properties at zero magnetic field. The weak confinement regime in the ferromagnetic 3-state PFT is discussed in Section 3, where the non-relativistic quantum three-body problem, which determines the masses of light baryons is also presented. In Section 4, we reduce this quantum three-body problem to the Fredholm integral equation, which numerical solution is described in Section 5. Concluding remarks are given in Section 6.

2. Potts field theory

The Potts field theory describes the scaling limit of the two-dimensional q -state Potts model with the number of colors q lying in the interval $q \leq 4$. The PFT Euclidean action can be written as [23, 5, 24]

$$\mathcal{A} = \mathcal{A}_{CFT}^{(q)} - \tau \int d^2x \varepsilon(x) - h \int d^2x \sigma_q(x), \quad (1)$$

Here $\mathcal{A}_{CFT}^{(q)}$ corresponds to the Conformal Field Theory, which is associated with the critical point, $\varepsilon(x)$ is the energy density, $\sigma_\alpha(x)$ are the spin densities, which are subject to the constrain $\sum_{\alpha=1}^q \sigma_\alpha(x) = 0$. The couplings τ and h are proportional to the deviation

of the temperature and magnetic field from their critical point values. The magnetic field h is chosen to act on the q -th color only. At the critical point, the energy density and the spin density have the scaling dimensions $X_\epsilon^{(q)}$, $X_\sigma^{(q)}$, respectively.

At $h = 0$, the Potts model is invariant under the permutation group S_q ; at $h \neq 0$ the symmetry reduces to the group S_{q-1} of permutations of the colors $\alpha = 1, \dots, q-1$. The PFT is integrable at $h = 0$. At $h = 0$ and $\tau < 0$, the S_q symmetry is spontaneously broken: the model has q degenerate vacua $|0_\alpha\rangle$, $\alpha = 1, 2, \dots, q$, which are distinguished by the values of the order parameter $\langle \sigma_\gamma \rangle_\alpha \equiv \langle 0_\alpha | \sigma_\gamma(x) | 0_\alpha \rangle$. The symmetry group S_q acts by permutations of these vacua.

In this paper, we shall concentrate on the PFT with $q = 3$ in the ordered phase $\tau < 0$. At $h = 0$ and $\tau < 0$, the 3-state PFT has three degenerate vacua $|0_\alpha\rangle$, $\alpha = 1, 2, 3$ shown schematically in Figure 1a. Its particle sector contains six kinks $K_{\alpha\beta}(\theta)$, $\alpha, \beta = 1, 2, 3$, which interpolate between two different vacua α and β , see Figure 1b. Each kink $K_{\alpha\beta}(\theta)$ is a relativistic particle having mass m and rapidity θ . The latter parametrizes the kink's energy $E = m \cosh \theta$ and momentum $p = m \sinh \theta$. The kink mass is related with the parameter τ as $|\tau| \sim m^{2-X_\epsilon^{(q)}}$.

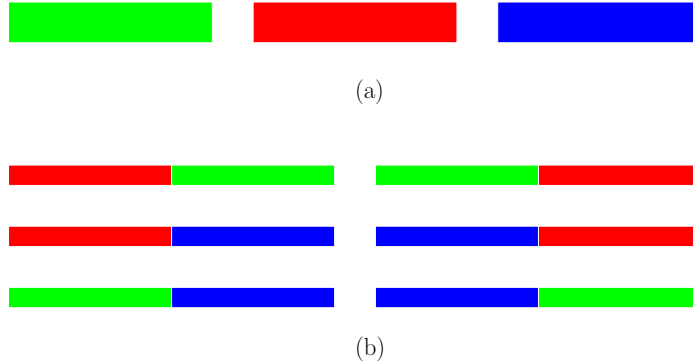


Figure 1. (a) Three degenerate vacua $|0_\alpha\rangle$, and (b) six kinks $K_{\alpha\beta}$, $\alpha, \beta = 1, 2, 3$ of the 3-state PFT at $\tau < 0$ and $h = 0$.

In contrast to the IFT, the kinks in the 3-state PFT interact with each other at distances $\lesssim m^{-1}$ already at $h = 0$. This interaction leads to the mutual kink scattering, which is described by the factorizable scattering matrix. The corresponding two-kink scattering matrix in the q -state PFT is described by the commutation relations found by Chim and Zamolodchikov [23]:

$$K_{\alpha\gamma}(\theta_1)K_{\gamma\beta}(\theta_2) = S_0(\theta_{12}) \sum_{\delta \neq \gamma} K_{\alpha\delta}(\theta_2)K_{\delta\beta}(\theta_1) \quad (2)$$

$$+ S_1(\theta_{12})K_{\alpha\gamma}(\theta_2)K_{\gamma\beta}(\theta_1), \quad \alpha \neq \beta, \\ K_{\alpha\gamma}(\theta_1)K_{\gamma\alpha}(\theta_2) = S_2(\theta_{12}) \sum_{\delta \neq \gamma} K_{\alpha\delta}(\theta_2)K_{\delta\alpha}(\theta_1) \quad (3) \\ + S_3(\theta_{12})K_{\alpha\gamma}(\theta_2)K_{\gamma\alpha}(\theta_1),$$

where $\theta_{1,2} = \theta_1 - \theta_2$, and

$$S_0(\theta) = \frac{\sinh \lambda \theta \sinh \lambda(\theta - i\pi)}{\sinh \lambda \left(\theta - \frac{2\pi i}{3}\right) \sinh \lambda \left(\theta - \frac{i\pi}{3}\right)} \Pi \left(\frac{\lambda \theta}{i\pi} \right), \quad (4)$$

$$S_1(\theta) = \frac{\sin \frac{2\pi\lambda}{3} \sinh \lambda(\theta - i\pi)}{\sin \frac{\pi\lambda}{3} \sinh \lambda \left(\theta - \frac{2i\pi}{3}\right)} \Pi \left(\frac{\lambda \theta}{i\pi} \right), \quad (5)$$

$$S_2(\theta) = \frac{\sin \frac{2\pi\lambda}{3} \sinh \lambda \theta}{\sin \frac{\pi\lambda}{3} \sinh \lambda \left(\theta - \frac{i\pi}{3}\right)} \Pi \left(\frac{\lambda \theta}{i\pi} \right), \quad (6)$$

$$S_3(\theta) = \frac{\sin \lambda \pi}{\sin \frac{\pi\lambda}{3}} \Pi \left(\frac{\lambda \theta}{i\pi} \right). \quad (7)$$

The parameter λ is related to q via

$$\sqrt{q} = 2 \sin \frac{\pi\lambda}{3}, \quad (8)$$

and

$$\Pi \left(\frac{\lambda \theta}{i\pi} \right) = \frac{\sinh \lambda \left(\theta + i\frac{\pi}{3}\right)}{\sinh \lambda(\theta - i\pi)} e^{A(\theta)}, \quad (9)$$

$$A(\theta) = \int_0^\infty \frac{dx}{x} \frac{\sinh \frac{x}{2} \left(1 - \frac{1}{\lambda}\right) - \sinh \frac{x}{2} \left(\frac{1}{\lambda} - \frac{5}{3}\right)}{\sinh \frac{x}{2\lambda} \cosh \frac{x}{2}} \sinh \frac{x\theta}{i\pi}. \quad (10)$$

Due to (8), the parameter λ takes the value unity in the 3-state PFT,

$$\lambda = 1, \quad \text{at } q = 3. \quad (11)$$

Note, that at $q = 3$, the scaling dimensions of the energy density and the spin density operators take the values [5]

$$X_\epsilon^{(3)} = \frac{4}{5}, \quad X_\sigma^{(3)} = \frac{2}{15}.$$

3. Weak confinement in the 3-state PFT

Application of a weak magnetic field $h > 0$ along the third direction decreases the energy of the vacuum $|0_3\rangle$, lifting the degeneracy between the vacuum $|0_3\rangle$ and the remaining ones $|0_{1,2}\rangle$. The vacuum $|0_3\rangle$ becomes the true ground state of the system, and the states $|0_{1,2}\rangle$ become false (metastable) vacua. In the leading order in h , the energy density difference between the ground state $|0_3\rangle$ and the metastable vacua $|0_{1,2}\rangle$ reads [5]

$$\Delta \mathcal{E} = \mathcal{E}_\alpha - \mathcal{E}_3 = f_0 + O(h^2), \quad \alpha = 1, 2, \quad (12)$$

$$f_0 = \frac{3bh}{2}, \quad (13)$$

with some positive b . This energy shift leads to a long-range linear attractive potential between kinks, which causes their confinement into mesonic and baryonic bound states [5]. There are two series of mesonic states $\pi_n^{(\kappa)}$,

$$\pi_n^{(\kappa)} = K_{31}K_{13} + (-1)^\kappa K_{32}K_{23},$$

and two series of baryonic states $p_n^{(\kappa)}$,

$$p_n^{(\kappa)} = K_{31}K_{12}K_{23} + (-1)^\kappa K_{32}K_{21}K_{13},$$

which differ by their parity $\kappa = 0, 1$, see Figure 2.

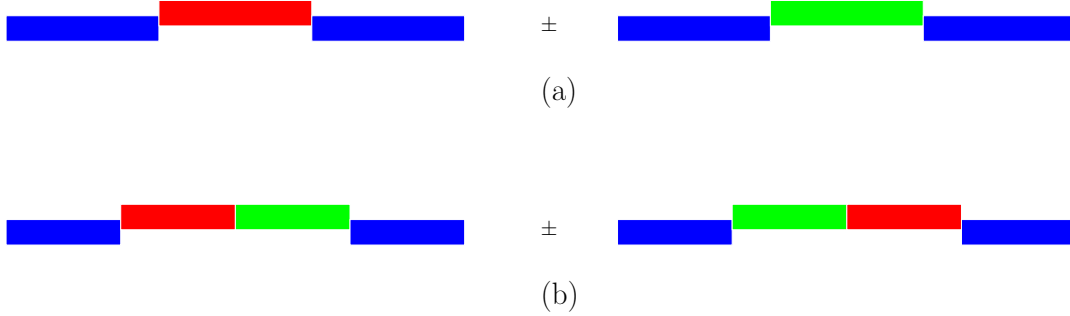


Figure 2. (a) Meson, and (b) baryon bound states of kinks in the 3-state PFT at $\tau < 0$ and a small $h > 0$.

It was shown in [25] that the masses of the lightest mesons $\mu_n^{(\kappa)}$, $n = 1, 2, \dots$, at small $h > 0$ can be determined to leading order in h from the Schrödinger eigenvalue problem

$$\left[-\frac{\partial_{x_1}^2}{2m} - \frac{\partial_{x_2}^2}{2m} + 2m - \mu_n^{(\kappa)} + (x_2 - x_1)f_0 \right] \psi_n^{(\kappa)}(x_1, x_2) = 0,$$

where $-\infty < x_1 < x_2 < \infty$, and f_0 is the string tension given by (13). The eigenfunction $\psi_n^{(\kappa)}(x_1, x_2)$ must be translationally invariant, i.e.,

$$\psi_n^{(\kappa)}(x_1, x_2) = \psi_n^{(\kappa)}(x_1 + X, x_2 + X) \quad \text{for all } X, \quad (14)$$

vanish fast enough at $(x_2 - x_1) \rightarrow +\infty$, and satisfy the boundary conditions

$$\begin{aligned} \psi_n^{(1)}(x_1, x_2)|_{x_1=x_2} &= 0, \\ (\partial_{x_1} - \partial_{x_2})\psi_n^{(0)}(x_1, x_2)|_{x_1=x_2} &= 0. \end{aligned}$$

It was shown in [25], that these boundary conditions follow from the small- θ asymptotics of the two-kink scattering matrix (2)-(7) at $q = 3$. The translation invariance requirement (14) guarantees, that the wave function $\psi_n^{(\kappa)}(x_1, x_2)$ describes the meson at rest.

The resulting mass spectrum of the light mesons reads [25]:

$$\begin{aligned} \mu_n^{(1)} &= 2m + f_0^{2/3} m^{-1/3} z_n + O(f_0^{4/3}), \\ \mu_n^{(0)} &= 2m + f_0^{2/3} m^{-1/3} z'_n + O(f_0^{4/3}), \end{aligned}$$

where $(-z_n)$ and $(-z'_n)$ are the zeroes of the Airy function $\text{Ai}(x)$ and its derivative $\text{Ai}'(x)$, respectively.

In order to determine the masses of the lightest baryons $M_n^{(\kappa)}$ at small $h > 0$, we shall apply a similar strategy. The subsequent analysis is essentially based on the experience gained from the perturbative study [3, 21] of the meson mass spectrum in the Ising field theory.

In leading order in $h \rightarrow +0$, the baryon can be treated as a bound state of three kinks, whereas the N -kink fluctuations with $N > 3$ should contribute to the baryon state at higher orders in h . In the three-kink approximation, the state $|B^{(\kappa)}(P)\rangle$ of a baryon having the momentum P and parity κ can be described in the position-space representation by the wave function

$$\begin{aligned} \Psi^{(\kappa)}(x_1, x_2, x_3; P) &= \langle K_{31}(x_1)K_{12}(x_2)K_{23}(x_3) | B^{(\kappa)}(P) \rangle = \\ &= (-1)^\kappa \langle K_{32}(x_1)K_{21}(x_2)K_{13}(x_3) | B^{(\kappa)}(P) \rangle, \end{aligned} \quad (15)$$

where x_α , $\alpha = 1, 2, 3$, are the spatial coordinates of the kinks,

$$\{x_1, x_2, x_3\} \in \Gamma \subset \mathbb{R}^3, \quad \Gamma = \{x_1, x_2, x_3 \in \Gamma | -\infty < x_1 < x_2 < x_3 < \infty\}. \quad (16)$$

The wave function (15) should vanish fast enough as $(x_3 - x_1) \rightarrow \infty$, and obey the following symmetry properties

$$\begin{aligned} \Psi^{(\kappa)}(x_1 + X, x_2 + X, x_3 + X; P) &= e^{iPX} \Psi^{(\kappa)}(x_1, x_2, x_3; P), \\ \Psi^{(\kappa)}(-x_3, -x_2, -x_1; -P) &= (-1)^\kappa \Psi^{(\kappa)}(x_1, x_2, x_3; P), \end{aligned} \quad (17)$$

for arbitrary X .

Since the masses $M_n^{(\kappa)}$ of baryons with small enough $n = 1, 2, \dots$ at $h \rightarrow +0$ only slightly exceed $3m$, $M_n^{(\kappa)} - 3m \sim h^{2/3}$, the kinetic energies of three kinks forming a baryon with zero momentum $P = 0$ should be small compared with their mass m . This allows one to treat such three kinks as non-relativistic quantum particles. These particles interact with each other with the linear potential

$$V(x_1, x_2, x_3) = (x_3 - x_1) f_0 \quad (18)$$

at large distances $(x_3 - x_1) \gg m^{-1}$. The above potential does not depend on the coordinate x_2 of the middle kink, which separates domains of the metastable phases 1 and 2 characterized by the same energy density $\mathcal{E}_1 = \mathcal{E}_2$, see Figure 2b.

Accordingly, the masses $M_n^{(\kappa)}$ of the lightest baryons $n = 1, 2, \dots$ can be determined in the leading order in $h \rightarrow +0$ from the three-particle Schrödinger partial differential equation

$$\left[-\sum_{j=1}^3 \frac{\partial^2}{\partial x_j^2} + 3m - M_n^{(\kappa)} + (x_3 - x_1)f_0 \right] \Psi_n^{(\kappa)}(x_1, x_2, x_3; 0) = 0, \quad (19)$$

in the domain (16). The boundary conditions for the wave function in the above equation at the planes $x_1 = x_2$ and $x_2 = x_3$ can be determined from the small- θ asymptotes of the scattering matrix, since the rapidities of kinks forming a light resting baryon are small. To this end, we need only the first commutation relation (2), which reduces at

$\alpha = q = 3$ to the form

$$K_{3\gamma}(\theta_1)K_{\gamma\beta}(\theta_2) = S_1(\theta_1 - \theta_2)K_{3\gamma}(\theta_2)K_{\gamma\beta}(\theta_1), \quad (20)$$

$$S_1(\theta) = -\exp \left[-2i \int_0^\infty \frac{dx}{x} \frac{\sinh(x/3)}{\sinh x} \sin(x\theta/\pi) \right], \quad (21)$$

with $\gamma \neq \beta$, and $\gamma, \beta \neq 3$. At small rapidity θ we get

$$S_1(\theta) = -1 + O(\theta), \quad (22)$$

$$K_{3\gamma}(\theta_1)K_{\gamma\beta}(\theta_2) = -K_{3\gamma}(\theta_2)K_{\gamma\beta}(\theta_1) + O(\theta_1 - \theta_2).$$

The 'free-fermionic' scattering matrix element (22), should induce the fermionic boundary conditions

$$\Psi_n^{(\kappa)}(x_1, x_2, x_3; 0)|_{x_1=x_2} = 0, \quad \Psi_n^{(\kappa)}(x_1, x_2, x_3; 0)|_{x_2=x_3} = 0 \quad (23)$$

for the baryon wave function in (19), as it was explained in [25] for the case of the meson wave functions.

For the baryon at rest, the symmetry properties (17) reduce to the form

$$\Psi^{(\kappa)}(x_1 + X, x_2 + X, x_3 + X; 0) = \Psi_P^{(\kappa)}(x_1, x_2, x_3; 0), \quad (24)$$

$$\Psi^{(\kappa)}(-x_3, -x_2, -x_1; 0) = (-1)^\kappa \Psi^{(\kappa)}(x_1, x_2, x_3; 0).$$

4. Reducing of the eigenvalue problem to the Fredholm integral equation

Let us proceed to the rescaled variables:

$$x_j = (mf_0)^{-1/3} \xi_j, \quad j = 1, 2, 3, \quad (25)$$

$$M_n^{(\kappa)} = 3m + f_0^{2/3} m^{-1/3} \epsilon_n^{(\kappa)}, \quad (26)$$

$$\Psi_n^{(\kappa)}(x_1, x_2, x_3; 0) = (mf_0)^{1/3} \Phi_n^{(\kappa)}(\xi_1, \xi_2, \xi_3). \quad (27)$$

Then, equation (19) takes the form

$$\left(-\frac{1}{2} \sum_{j=1}^3 \partial_{\xi_j}^2 - \epsilon_n^{(\kappa)} + \xi_3 - \xi_1 \right) \Phi_n^{(\kappa)}(\xi_1, \xi_2, \xi_3) = 0, \quad (28)$$

for $-\infty < \xi_1 < \xi_2 < \xi_3 < \infty$. We shall use the following Ansatz for the solution of this equation:

$$\Phi_n^{(\kappa)}(\xi_1, \xi_2, \xi_3) = \int_0^\infty dp g^{(\kappa)}(p) f^{(\kappa)} \left[p \left(\xi_2 - \frac{\xi_1 + \xi_3}{2} \right) \right] \text{Ai} \left(\xi_3 - \xi_1 + \frac{3p^2}{4} - \epsilon_n^{(\kappa)} \right), \quad (29)$$

where $f^{(0)}(z) = \cos z$, $f^{(1)}(z) = \sin z$, $\text{Ai}(\xi)$ is the Airy function, and $g^{(\kappa)}(p)$ is some unknown function.

One can easily check, that the right-hand side of (29) with an arbitrary function $g^{(\kappa)}(p)$ providing convergence of the integral in p gives a solution of equation (28). The function $\Phi_n^{(\kappa)}(\xi_1, \xi_2, \xi_3)$ defined by (29) also satisfies the equalities

$$\Phi^{(\kappa)}(\xi_1 + \xi, \xi_2 + \xi, \xi_3 + \xi) = \Phi^{(\kappa)}(\xi_1, \xi_2, \xi_3), \quad \xi \in \mathbb{R}, \quad (30)$$

$$\Phi^{(\kappa)}(-\xi_3, -\xi_2, -\xi_1) = (-1)^\kappa \Phi^{(\kappa)}(\xi_1, \xi_2, \xi_3),$$

which guarantee (24).

We require, further, that $\Phi^{(\kappa)}(\xi_1, \xi_2, \xi_3)$ vanishes fast enough as $(\xi_3 - \xi_1) \rightarrow +\infty$ in the domain $-\infty < \xi_1 < \xi_2 < \xi_3 < \infty$. To satisfy also the boundary condition (23), one ought to require that the function $g^{(\kappa)}(p)$ is the solution of the linear homogeneous integral equation

$$\int_0^\infty dp U^{(\kappa)}(\xi, p; \epsilon_n^{(\kappa)}) g^{(\kappa)}(p) = 0 \quad (31)$$

on the half-line $0 < \xi < \infty$, with the asymmetric kernel

$$U^{(\kappa)}(\xi, p; \epsilon) = f^{(\kappa)}(p \xi/2) \text{Ai} \left(\xi + \frac{3p^2}{4} - \epsilon \right). \quad (32)$$

After the change of variables

$$\begin{aligned} \xi &= \frac{u}{1-u}, \quad p = \left[\frac{4v}{3(1-v)} \right]^{1/2}, \\ g^{(\kappa)}(p) &= \phi^{(\kappa)}(v) (3v)^{1/2} (1-v)^{3/2}, \end{aligned} \quad (33)$$

the integral equation (31) takes the form

$$\int_0^1 dv K^{(\kappa)}(u, v; \epsilon_n^{(\kappa)}) \phi^{(\kappa)}(v) = 0, \quad (34)$$

for $0 \leq u \leq 1$, whose kernel

$$K^{(\kappa)}(u, v; \epsilon) = f^{(\kappa)} \left(\frac{u v^{1/2}}{(1-u)[3(1-v)]^{1/2}} \right) \text{Ai} \left(\frac{u}{1-u} + \frac{v}{1-v} - \epsilon \right) \quad (35)$$

is continuous in the square $0 \leq u, v \leq 1$.

Consider the Fredholm operator eigenvalue problem [28]:

$$\int_0^1 dv K^{(\kappa)}(u, v; \epsilon) g_\nu^{(\kappa)}(v; \epsilon) = \lambda_\nu^{(\kappa)}(\epsilon) g_\nu^{(\kappa)}(u, \epsilon). \quad (36)$$

For arbitrary complex ϵ , the spectrum $\lambda_\nu^{(\kappa)}(\epsilon)$, $\nu = 1, 2, \dots, \infty$ is discrete with the limiting point $\lambda_\nu^{(\kappa)}(\epsilon) \rightarrow 0$ at $\nu \rightarrow \infty$. The baryon masses $M_n^{(\kappa)}$, $n = 1, 2, \dots$ are determined through (26) by the solutions of the equation

$$\lambda_{\nu(n)}^{(\kappa)}(\epsilon)|_{\epsilon=\epsilon_n^{(\kappa)}} = 0, \quad (37)$$

with some $\nu(n)$.

5. Numerical solution of equation (37)

For the numerical solution, the Fredholm integral operator in equation (36) was replaced by the ϵ -dependent square $N \times N$ -matrix $\mathcal{K}_{ij}^{(\kappa)}(\epsilon, N)$,

$$\begin{aligned} \mathcal{K}_{ij}^{(\kappa)}(\epsilon, N) &= \frac{K^{(\kappa)}(u_i, v_j; \epsilon)}{N}, \\ u_i &= \frac{i}{N-1}, \quad v_j = \frac{j}{N-1}, \quad i, j = 0, 1, 2, \dots, N-1. \end{aligned} \quad (38)$$

In the limit $N \rightarrow \infty$, eigenvalues $\Lambda_\nu^{(\kappa)}(\epsilon, N)$ of this matrix should approach the eigenvalues of the Fredholm integral equation (36),

$$\lim_{N \rightarrow \infty} \Lambda_\nu^{(\kappa)}(\epsilon, N) = \lambda_\nu^{(\kappa)}(\epsilon). \quad (39)$$

The matrix $\mathcal{K}_{ij}^{(\kappa)}(\epsilon, N)$ was diagonalized numerically for given N . The evolution of its eigenvalues upon increasing ϵ is plotted in Figure 3 for the matrix dimensions $N = 31$ and $N = 101$. For complex eigenvalues, both real and imaginary parts are displayed.

The obtained numerical results indicate a very fast decrease of the absolute values of the eigenvalue $\Lambda_\nu^{(\kappa)}(\epsilon, N)$ with increasing ν , at fixed ϵ and N . For $\epsilon = 0$, this is illustrated in Table 1. Accordingly, only two eigenvalues corresponding to $\nu = 1, 2$ can be distinguished from zero in Figure 3 at $\epsilon = 0$. As soon as ϵ increases, subsequent eigenvalues with $\nu = 3, 4, \dots$ become larger in absolute values, deviating one by one from the abscisses in Figures 3a,b.

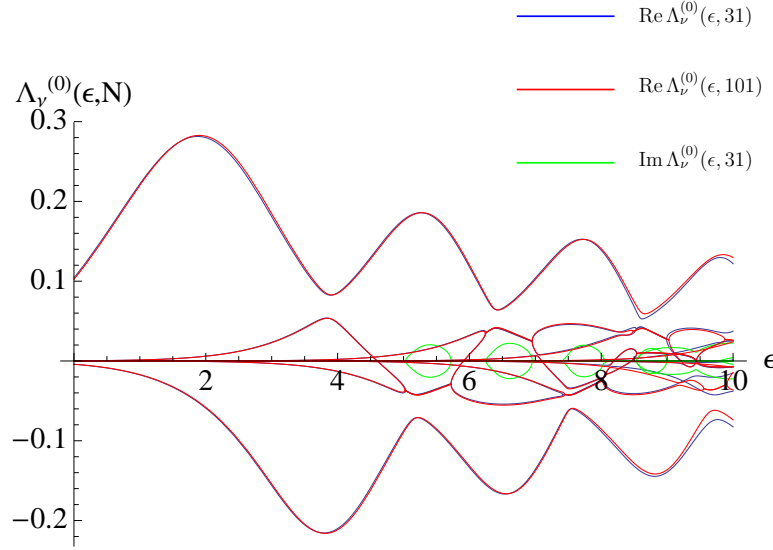
Another important feature of the spectral patterns shown in Figure 3 is that the blue and red curves, which correspond to the matrix dimensions $N = 31$, and $N = 101$, respectively, remain rather close to each other at small enough $\epsilon \lesssim 8$. Due to (39), one should expect, that these patterns are also close to the asymptotical $N \rightarrow \infty$ spectra, i.e. to the spectra $\lambda_{\nu(n)}^{(\kappa)}(\epsilon)$ of the Fredholm integral equation (36).

However, the eigenvalue $\Lambda_\nu^{(\kappa)}(\epsilon, N)$ approaches its limiting values $\lambda_\nu^{(\kappa)}(\epsilon)$ for $N \rightarrow \infty$ not uniformly in ϵ : at larger ϵ one has to proceed to larger matrix dimensions N to reach the asymptotic $N \rightarrow \infty$ value. The reason is that the large positive ϵ shifts the argument $z = \left(\frac{u}{1-u} + \frac{v}{1-v} - \epsilon\right)$ of the Airy function $\text{Ai}(z)$ in the integral kernel (35) to negative z . Since $\text{Ai}(z)$ oscillates at negative z , the kernel $K^{(\kappa)}(u, v; \epsilon)$ becomes strongly oscillating in the square $0 < u, v < 1$ at large ϵ . Therefore, as ϵ increases, one should proceed to larger matrix dimensions N in order to provide 'sufficient resolution' to approximate the highly oscillating kernel $K^{(\kappa)}(u, v; \epsilon)$ in the square $0 < u, v < 1$ by its $N \times N$ -discrete-lattice counterpart $\mathcal{K}_{ij}^{(\kappa)}(\epsilon, N)$.

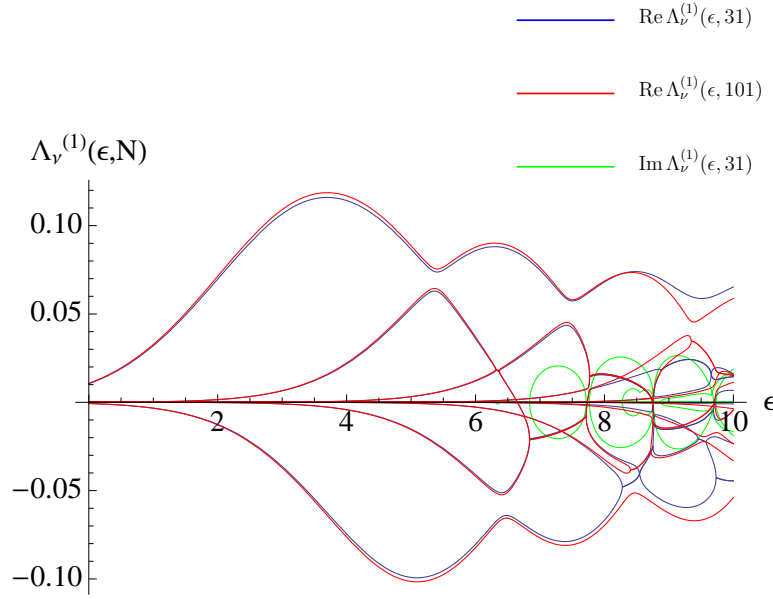
The deviations between the blue ($N = 31$) and red ($N = 101$) curves in Figures 3a,b become considerable at $\epsilon \simeq 9$ and increase further at larger ϵ . This indicates that at such large $\epsilon \gtrsim 9$ one has to increase the matrix dimension N to higher values to be able to describe the $N \rightarrow \infty$ asymptotic spectrum $\lambda_\nu^{(\kappa)}(\epsilon)$.

ν	1	2	3	4
$\Lambda_\nu^{(0)}(0, 31)$	0.104289	-0.00416232	0.000225285	-0.0000140359
$\Lambda_\nu^{(0)}(0, 101)$	0.102381	-0.00407641	0.000220799	-0.0000137643
$\Lambda_\nu^{(1)}(0, 31)$	0.0104795	-0.000685642	0.0000447833	-3.02246×10^{-6}
$\Lambda_\nu^{(1)}(0, 101)$	0.0107229	-0.000701738	0.0000458517	-3.09608×10^{-6}

Table 1. Four initial eigenvalues $\Lambda_\nu^{(\kappa)}(0, N)$ of the $N \times N$ -matrices $\mathcal{K}_{ij}^{(\kappa)}(\epsilon, N)$ at $\epsilon = 0$ for $N = 31, 101$ and $\kappa = 0, 1$.



(a)



(b)

Figure 3. Evolution of the eigenvalues of the discretized versions of the Fredholm integral equation (36) with increasing ϵ with matrix dimensions $N = 31$, and $N = 101$ for the baryon parities (a) $\kappa = 0$, and (b) $\kappa = 1$.

Several crossings of the ϵ -axis by the spectral curves are clearly seen in Figures 3a,b. The first three ones are located at

$$\epsilon_1^{(0)} = 4.602, \quad \epsilon_2^{(0)} = 5.912, \quad \epsilon_3^{(0)} = 7.098, \quad (40)$$

for $\kappa = 0$ in Figure 3a, and at

$$\epsilon_1^{(1)} = 6.650, \quad \epsilon_2^{(1)} = 7.734, \quad \epsilon_3^{(1)} = 8.753, \quad (41)$$

for $\kappa = 1$ in Figure 3b. Up to the digits specified in (40) and (41), the locations of these crossing points for red and blue curves coincide. Accordingly, we finally get from (26) the masses of the lightest baryons at $h \rightarrow +0$:

$$M_n^{(\kappa)} = 3m + f_0^{2/3} m^{-1/3} \epsilon_n^{(\kappa)} + O(f_0^{4/3}), \quad \text{with } \kappa = 0, 1, \quad n = 1, 2, 3, \dots, \quad (42)$$

where $\epsilon_n^{(\kappa)}$ for $\nu = 1, 2, 3$ are given by equations (40), (41).

It should be noted that before crossing the ϵ -axis, the spectral curve $\lambda_\nu^{(\kappa)}(\epsilon)$ crosses infinitely many other spectral curves $\lambda_{\nu'}^{(\kappa)}(\epsilon)$ with large enough ν' , since

$$\lim_{\nu' \rightarrow \infty} \lambda_{\nu'}^{(\kappa)}(\epsilon) = 0.$$

In fact, such crossings between two spectral curves $\lambda_\nu^{(\kappa)}(\epsilon)$ and $\lambda_{\nu'}^{(\kappa)}(\epsilon)$ are rather avoided crossings, or turning points of the spectral curves. All these features can be seen in

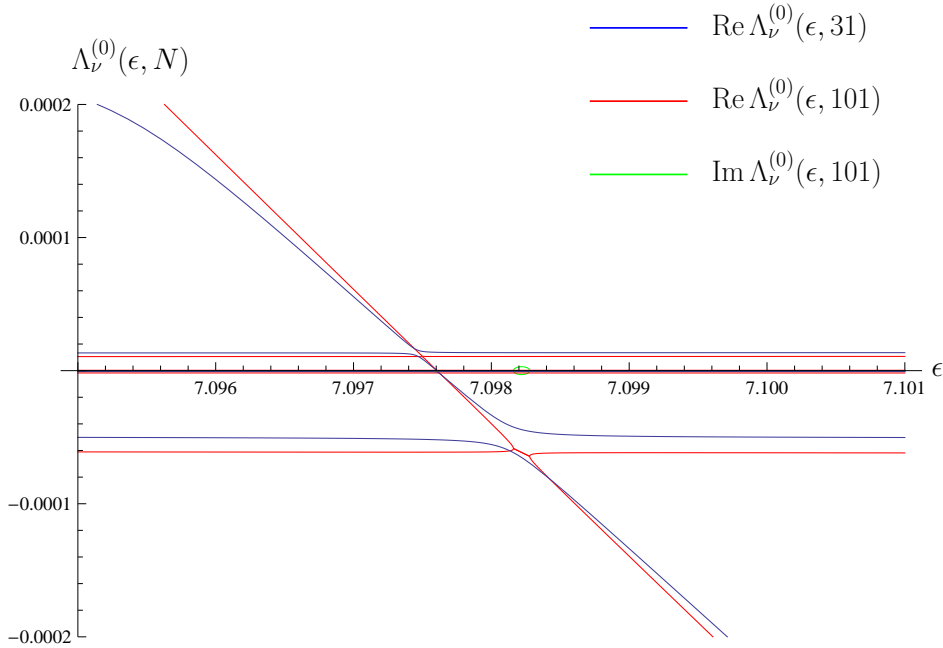


Figure 4. The fine structure of the spectral curves $\Lambda_\nu^{(0)}(\epsilon, N)$ near the point $\epsilon \approx \epsilon_3^{(0)}$. The blue curves corresponding to the matrix dimension $N = 31$ display avoided crossing near the point $\epsilon = 7.0982$, which transforms into two turning points in red curves relating to the case $N = 101$. Between these two turning points, corresponding two eigenvalues become complex and mutually conjugate.

Figure 4, which displays the evolution of the spectral curves $\Lambda_\nu^{(0)}(\epsilon, N)$ for $N = 31, 101$ in the small region near the third crossing point $\epsilon \approx \epsilon_3^{(0)} = 7.098\dots$

6. Conclusions

In this paper we have studied the baryonic excitations in the 3-state Potts field theory in the weak confinement regime, which is realized in the ordered phase in the presence of a weak magnetic field h acting on the third color. Two series of baryons with parities $\kappa = 0, 1$ are allowed, if the applied magnetic field is positive, i.e. if the resulting ground state $|0_3\rangle$ becomes non-degenerate in energy.

To determine the masses of the light baryons in the regime of small magnetic field h , we have applied the procedure that was originally developed to calculate the meson masses in the IFT [20, 2], and has been used later [25] for meson mass calculations in the PFT. In this approach, the baryon (or the meson) is interpreted as a bound state of three (or two) kinks, which are treated as non-relativistic interacting quantum particles. The light baryon mass spectrum was determined from the stationary Schrödinger equation, which describes relative one-dimensional motion of three kinks with coordinates $-\infty < x_1 < x_2 < x_3 < \infty$ interacting via the linear confining potential $(x_3 - x_1)f_0$. Here $f_0 > 0$ is the string tension, which is proportional to the applied magnetic field h . The boundary condition for the Schrödinger equation at $x_1 = x_2$ and $x_2 = x_3$ were gained from the low-momentum asymptotics of the exactly known two-kink scattering matrix [23] at $h = 0$. The resulting mass spectrum of the light baryons in the leading order in $h \rightarrow +0$ is given by equation (42). Several coefficients $\epsilon_n^{(\kappa)}$, with $\kappa = 1, 2$, and $n = 1, 2, 3$ in this equation were obtained numerically, see equations (40), (41).

Note, that the employed procedure is well justified in the case of the meson mass spectrum in the IFT, since it reproduces the leading order of the low-energy expansion (see equation (5.16) in reference [3]), which was derived in the systematic perturbative approach based on the Bethe-Salpeter equation [2, 3].

As it was shown in [24], the numerical TCSA method provides an alternative possibility to study the baryon mass spectra in the 3-state PFT. It would be interesting to perform systematic TCSA calculations of the baryon masses in this model at small magnetic fields, and to compare the TCSA baryon spectra with our results.

Acknowledgments

I am thankful to H. W. Diehl for interesting discussions and numerous suggestions leading to improvement of the text.

This work was supported by Deutsche Forschungsgemeinschaft (DFG) via Grant Ru 1506/1.

References

- [1] G. Delfino and G. Mussardo. Non-integrable aspects of the multi-frequency sine-Gordon model. *Nucl. Phys. B*, 516(3):675–703, 1998. (*Preprint* hep-th/9709028).

- [2] P. Fonseca and A. Zamolodchikov. Ising field theory in a magnetic field: Analytic properties of the free energy. *J. Stat. Phys.*, 110(3-6):527–590, 2003.
- [3] P. Fonseca and A. Zamolodchikov. Ising spectroscopy I: Mesons at $T < T_c$. 2006. arXiv:hep-th/0612304.
- [4] S. B. Rutkevich. Large- n excitations in the ferromagnetic Ising field theory in a weak magnetic field: Mass spectrum and decay widths. *Phys. Rev. Lett.*, 95(25):250601, 2005. (Preprint hep-th/0509149).
- [5] G. Delfino and P. Grinza. Confinement in the q -state Potts field theory. *Nucl. Phys. B*, 791(3):265–283, 2008. (Preprint hep-th/0706.1020).
- [6] G. Mussardo and G. Takács. Effective potentials and kink spectra in non-integrable perturbed conformal field theories. *J. Phys. A*, 42(30):304022, 2009.
- [7] G. Mussardo. Integrability, non-integrability and confinement. *Journal of Statistical Mechanics: Theory and Experiment*, 2011(01):P01002, 2011.
- [8] A. Zamolodchikov and I. Ziyatdinov. Inelastic scattering and elastic amplitude in Ising field theory in a weak magnetic field at $T > T_c$. Perturbative analysis. *Nuclear Physics B*, 849(3):654 – 674, 2011.
- [9] A. Zamolodchikov. Ising spectroscopy II: Particles and poles at $T > T_c$. 2013. arXiv:1310.4821.
- [10] S. B. Rutkevich. Analytic verification of the droplet picture in the two-dimensional Ising model. *J. Stat. Phys.*, 104(3/4):589–608, 2001. (Preprint cond-mat/0008033).
- [11] V. V. Mangazeev, M. Yu. Dudalev, V. V. Bazhanov, and M. T. Batchelor. Scaling and universality in the two-dimensional Ising model with a magnetic field. *Phys. Rev. E*, 81(6):060103, 2010.
- [12] G. P. Brandino, R. M. Konik, and G. Mussardo. Energy level distribution of perturbed conformal field theories. *J. Stat. Mech.*, P07013, 2010. (Preprint arXiv:1004.4844).
- [13] S. K. Ma. *Modern Theory of Critical Phenomena*. W. A. Benjamin, Advanced Book Program, 1976.
- [14] J. Cardy. *Scaling and Renormalization in Statistical Physics*. Cambridge Lecture Notes in Physics. Cambridge University Press, 1996.
- [15] G. 't Hooft. A two-dimensional model for mesons. *Nucl. Phys. B*, 75(3):461–470, 1974.
- [16] V. A. Fateev, S. L. Lukyanov, and A. B. Zamolodchikov. On the mass spectrum in 't Hooft's 2D model of mesons. *J. Phys. A*, 42(30):304012, 2009.
- [17] R. Coldea, D. A. Tennant, E. M. Wheeler, E. Wawrzynska, D. Prabhakaran, M. Telling, K. Habicht, P. Smeibidl, and K. Kiefer. Quantum criticality in an Ising chain: Experimental evidence for emergent E8 symmetry. *Science*, 327(5962):177–180, 2010.
- [18] C. M. Morris, R. V. Aguilar, A. Ghosh, S. M. Koochpayeh, J. Krizan, R. J. Cava, O. Tchernyshyov, T. M. McQueen, and N. P. Armitage. Hierarchy of bound states in the one-dimensional ferromagnetic Ising chain CoNb_2O_6 investigated by high-resolution time-domain terahertz spectroscopy. *Phys. Rev. Lett.*, 112:137403, Apr 2014.
- [19] S. Sachdev. *Quantum Phase Transitions*. Cambridge University Press, Cambridge, 1999.
- [20] B. M. McCoy and T. T. Wu. Two dimensional Ising field theory in a magnetic field: Breakup of the cut in the two-point function. *Phys Rev. D*, 18(4):1259–1267, 1978.
- [21] S. B. Rutkevich. Formfactor perturbation expansions and confinement in the Ising field theory. *J. Phys. A*, 42(30):304025, 2009. (Preprint arXiv:0901.1571).
- [22] R. J. Baxter. *Exactly Solved Models in Statistical Mechanics*. Academic Press, London, 1982.
- [23] L. Chim and A. B. Zamolodchikov. Integrable field theory of the q -state Potts model with $0 < q < 4$. *Int. J. Mod. Phys. A*, 7(21):5317–5336, 1992.
- [24] L. Lepori, G. Z. Tóth, and G. Delfino. The particle spectrum of the three-state Potts field theory: a numerical study. *J. Stat. Mech.*, P11007, 2009. (Preprint arXiv:0909.2192v2).
- [25] S. B. Rutkevich. Two-kink bound states in the magnetically perturbed Potts field theory at $T < T_c$. *J. Phys. A*, 42(23):304025, 2009. (Preprint arXiv:0907.3697v2).
- [26] V. P. Yurov and A. B. Zamolodchikov. Truncated-fermionic-space approach to the critical 2d Ising model with magnetic field. *Int. J. Mod. Phys. A*, 6(25):4557–4578, 1991.

- [27] M. Lencsés and G. Takács. Excited state TBA and renormalized TCSA in the scaling Potts model. 2014. arXiv:1405.3157.
- [28] M. Reed and B. Simon. *I: Functional Analysis*. Methods of Modern Mathematical Physics. Elsevier Science, 1981.